

# Characterization of $^{18}\text{F}$ -FDG Uptake in Human Endothelial Cells In Vitro

Simone Maschauer; Olaf Prante, PhD; Markus Hoffmann; J. Thiess Deichen, MD; and Torsten Kuwert, MD

*Department of Nuclear Medicine, Laboratory of Molecular Imaging, Friedrich-Alexander University, Erlangen, Germany*

The contribution of  $^{18}\text{F}$ -FDG uptake by endothelial cells to uptake values measured by PET in various tissues is as yet unclear. We therefore sought to characterize  $^{18}\text{F}$ -FDG uptake in an in vitro model of human endothelial cells. **Methods:** Commercially obtained human umbilical vein endothelial cells (HUVECs) were seeded in 6-multiwell plates 48–96 h before incubation with 1–2 MBq  $^{18}\text{F}$ -FDG per well. Radioactivity measurements were performed after washing and mechanical dissolution of the cellular monolayers. Cellular  $^{18}\text{F}$ -FDG uptake was referred to protein concentration. This experimental protocol was subsequently varied to study the effect of different parameters of interest. Furthermore, radio-thin-layer chromatography was used to identify intracellular  $^{18}\text{F}$ -FDG metabolites.  $^{18}\text{F}$ -FDG uptake in HUVECs was compared with that by a human monocyte-macrophage (HMM) preparation and by glioblastoma cells (GLIOs) under identical experimental conditions. **Results:**  $^{18}\text{F}$ -FDG accumulated in HUVECs in a time-dependent manner and was trapped mainly as  $^{18}\text{F}$ -FDG-6-phosphate and  $^{18}\text{F}$ -FDG-1,6-diphosphate. Unlabeled glucose and cytochalasin B competitively inhibited  $^{18}\text{F}$ -FDG uptake, whereas phlorizin had no significant effect. Glucose deprivation significantly enhanced  $^{18}\text{F}$ -FDG uptake by a factor of 2.7, whereas sodium depletion had no significant influence. HUVECs treated with vascular endothelial growth factor (VEGF) showed a significant 82% increase in  $^{18}\text{F}$ -FDG accumulation after a 2-h exposure to 50 ng/mL VEGF.  $^{18}\text{F}$ -FDG uptake in HUVECs was significantly higher than that in HMMs and in the range of the uptake values measured in GLIOs. **Conclusion:**  $^{18}\text{F}$ -FDG accumulates in HUVECs by mechanisms analogous to those in neoplastic cells or neurons. VEGF significantly stimulates endothelial  $^{18}\text{F}$ -FDG uptake. The observed differences in  $^{18}\text{F}$ -FDG uptake between HUVECs, HMMs, and GLIOs are difficult to extrapolate to in vivo conditions but stimulate further studies on the contribution of endothelial  $^{18}\text{F}$ -FDG uptake to the overall uptake of that tracer in neoplastic or vascular lesions.

**Key Words:**  $^{18}\text{F}$ -FDG; glucose transport; endothelium; human umbilical vein endothelial cells; vascular endothelial growth factor

**J Nucl Med 2004; 45:455–460**

A valuable diagnostic tool in oncology is PET with  $^{18}\text{F}$ -FDG (1). However,  $^{18}\text{F}$ -FDG accumulates not only in neoplastic cells but also in inflammatory cells such as macrophages and lymphocytes, which potentially reduces diagnostic specificity (2–4).

The stimulation of angiogenesis is a prerequisite to tumor growth (5). Furthermore, microvessel density has been proven to be an indicator of higher malignancy for various types of tumors (6). Recently, a significant and positive correlation between microvessel density and  $^{18}\text{F}$ -FDG uptake has been reported in breast cancer (7). Occasionally, vessels are visualized on  $^{18}\text{F}$ -FDG PET images, for example, in vasculitis or atherosclerosis (8,9). The increased  $^{18}\text{F}$ -FDG uptake in vessels is usually ascribed to that in activated macrophages (3). However, since endothelial proliferation is induced by angiogenic factors released by activated macrophages (10),  $^{18}\text{F}$ -FDG uptake in endothelia may also contribute to this phenomenon.

As yet, little is known about the magnitude and mechanisms of  $^{18}\text{F}$ -FDG uptake in endothelial cells compared with tumor cells and macrophages. The aim of this study was therefore to characterize the uptake of  $^{18}\text{F}$ -FDG in an established in vitro model of human endothelial cells.

## MATERIALS AND METHODS

### Cell Culture Reagents and Chemicals

Endothelial basal medium, endothelial growth supplements (EGM-2-MV BulletKit: human epidermal growth factor [hEGF], hydrocortisone, fetal bovine serum [FBS], vascular endothelial growth factor [VEGF], human fibroblast growth factor-B [hFGF-B], recombinant 3 insulin-like growth factor [ $\text{R}^3$ -IGF-1], ascorbic acid, GA-1000), trypsin neutralizing solution, and Hanks' balanced salt solutions were purchased from Cambrex Bio Science. Glucose-free cell culture medium (Dulbecco's modified Eagle medium [DMEM], without glucose), fetal calf serum (FCS), phosphate-buffered saline (PBS), and trypsin/ethylenediaminetetraacetic acid were obtained from Invitrogen. D-Glucose, cytochalasin B, phlorizin, Bradford reagent, and vascular endothelial growth factor (VEGF<sub>165</sub>) were supplied by Sigma-Aldrich. Monoclonal antivascular endothelial growth factor receptor-2 (mouse) was obtained from Sigma.  $^{18}\text{F}$ -FDG was obtained from PET Net GmbH. For metabolic studies, radio-thin layer chromatography (radio-TLC) was performed on silica gel-coated plastic sheets

Received Aug. 4, 2003; revision accepted Oct. 15, 2003.  
For correspondence or reprints contact: Olaf Prante, PhD, University of Erlangen-Nürnberg, Department of Nuclear Medicine, Laboratory of Molecular Imaging, Schwabachanlage 6, D-91054 Erlangen, Germany.  
E-mail: olaf.prante@nuklear.imed.uni-erlangen.de

(Polygram SIL G/UV<sub>254</sub>; Macherey-Nagel). All other chemicals were commercially available and of analytic grade.

### Cell Culture of Human Umbilical Vein Endothelial Cells

The human umbilical vein endothelial cells (HUVECs) used in this study were obtained from Cambrex Bio Science. These cells were pooled from several human donors. Approximately  $2 \times 10^5$  HUVECs were plated in 75-mm<sup>2</sup> plastic culture bottles. Cells were cultured in a humidified atmosphere of 5% CO<sub>2</sub> at 37°C using an endothelial growth medium (EGM) containing the following supplements (SingleQuots; Cambrex Bio Science: 1 mL/L hEGF, 0.4 mL/L hydrocortisone, 50 mL/L FBS, 1 mL/L VEGF, 4 mL/L hFGF-B (with heparin), 1 mL/L R<sup>3</sup>-IGF-1, 1 mL/L ascorbic acid, 1 mL/L GA-1000. The final serum concentration in EGM was 5%. HUVECs were routinely subcultured every 4 d. Approximately 85,000 cells were seeded in 6-multiwell plates 48–96 h before experimental use.

### Cell Culture of Human Monocyte–Macrophages and Glioblastoma Cells

Human mononuclear cells were isolated from healthy human subjects by density gradient centrifugation using Ficoll methods, and macrophages were derived during cell culture (HMM = human monocyte–macrophage). Further purification, induction of differentiation, quality control, and handling were exactly as described previously (3). The human glioblastoma cell (GLIO) line U-138 MG was obtained from the American Type Culture Collection and handled as described previously (3).

### Immunocytochemical Staining

Twenty thousand cells in EGM were seeded in 8-well chamber slides (Nunc). After 24 h, immunocytochemical staining was performed using the universal Dako-APAAP kit following the instructions of the manufacturer. Monoclonal antivascular endothelial growth factor receptor-2 (KDR; clone KDR-2) from mouse was used as the primary antibody in a dilution of 1:80. Negative control slides were obtained by omitting the primary antibody.

### Determination of <sup>18</sup>F-FDG Uptake

One to 2 MBq <sup>18</sup>F-FDG were added to each culture well containing 1.2 mL of the incubation buffer, and incubation was continued for 3 h unless otherwise indicated. Incubation temperature was 4°C to allow the usage of PBS as the incubation buffer. After incubation, an aliquot of the incubation medium (50 µL) was used for radioactivity measurement. The incubation was terminated by rapidly pouring off the incubation buffer and rinsing the monolayer twice with 1.5 mL PBS. Cells were dissolved from the wells mechanically. The resulting cell suspension was used for radioactivity measurement (Caprac Counter; Capintec). After homogenization, determination of protein concentration was performed by the method of Bradford (11).

The following parameters were investigated:

- Incubation time: The incubation time was varied between 30 min and 3 h.
- Glucose concentration: The glucose concentration of the incubation buffer was varied between 0.2 and 200 mmol/L.
- Phlorizin concentration: The concentration of phlorizin, the classic competitive inhibitor of SGLT-1 (a sodium glucose cotransporter), in the incubation buffer was varied between 0.05 and 50 µmol/L.
- Cytochalasin B: The concentration of cytochalasin B, a facilitative glucose transporter (GLUT1–GLUT5) inhibitor, was varied between 0.01 and 5 µmol/L.

- Sodium depletion: Sodium-independent uptake was determined by substituting choline for sodium in the incubation buffer (sodium-free buffer: 0.2 g/L KH<sub>2</sub>PO<sub>4</sub>, 0.2 g/L KCl, 20.2 g/L choline chloride, pH 7.4)
- Preincubation of HUVECs with VEGF: To determine the effect of VEGF stimulation, cells were seeded in 12-multiwell plates and medium was changed to 0.8 mL EGM (2% FCS) 13 h before further experimental use. Cells were treated with VEGF (50 ng/mL) for 2 h at 37°C. The medium was removed and cells were tempered at 4°C in PBS for 15 min before determination of <sup>18</sup>F-FDG uptake.
- Glucose deprivation: Twenty hours before each experiment, cells were washed twice with cold PBS (1.5 mL) and the medium was changed to glucose-free medium (DMEM, without glucose) with 2% FCS.

### Radio-TLC

<sup>18</sup>F-FDG metabolites in HUVECs were investigated by radio-TLC on silica gel-coated plastic sheets (Polygram SIL G/UV<sub>254</sub>; Macherey-Nagel) with acetonitrile/tetrabutylammonium hydroxide, 9.5 mmol/L, 8:2 (v/v), as eluant. Chromatograms were measured using the InstantImager (Canberra Packard), and metabolites were identified by their R<sub>f</sub> values as described earlier (12).

### Statistics

All experiments were performed in triplicate unless otherwise indicated and repeated at least twice. Data are expressed as mean ± SD. The significance of differences in means was assessed using the Student *t* test subsequent to using the *F*-test for analyzing the equality of variances. The *F*-test was performed as a 1-way analysis of variances according to Levene (13).

## RESULTS

<sup>18</sup>F-FDG uptake in HUVECs expressed as the percentage injected dose per mg protein varied considerably between experimental assays ( $70.1 \pm 40.7$  %/mg;  $n = 22$ ). However, <sup>18</sup>F-FDG uptake values showed little within-assay variation, with a coefficient of variation (COV) of  $10.3\% \pm 6.8\%$  ( $n = 6$ ).

<sup>18</sup>F-FDG accumulation in HUVECs was shown to be a linear function of incubation time, which depicted a cellular uptake at 3 h roughly doubling that at 1.5 h (data not shown).

At 3 h of incubation, <sup>18</sup>F-FDG was intracellularly trapped mainly as <sup>18</sup>F-FDG-6-phosphate and <sup>18</sup>F-FDG-1,6-diphosphate analyzed by radio-TLC. The distribution of these radiolabeled compounds was as follows: <sup>18</sup>F-FDG-1,6-diphosphate/<sup>18</sup>F-FDG-6-phosphate/<sup>18</sup>F-FDG = 24:58:18 (percentage sum of regions) (Fig. 1).

Unlabeled glucose competitively inhibited <sup>18</sup>F-FDG uptake with concentrations of 20 mmol/L almost completely suppressing uptake (Table 1).

Phlorizin did not influence the <sup>18</sup>F-FDG uptake in HUVECs at concentrations between 0.05 and 50 µmol/L (Fig. 2), whereas cytochalasin B had the same effect on glucose uptake as unlabeled glucose (Fig. 3). Cytochalasin B competitively inhibited <sup>18</sup>F-FDG uptake with an inhibitory concentration of 50% (IC<sub>50</sub>) of 0.16 µmol/L (Fig. 3).

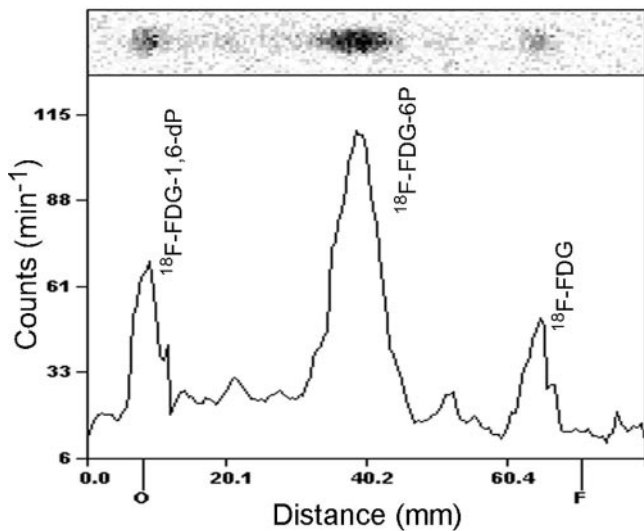


**FIGURE 1.** Radio-TLC of intracellular metabolites of  $^{18}\text{F}$ -FDG in HUVECs. Radio-TLC was performed on silica gel-coated plastic sheets with acetonitrile/tetrabutylammonium hydroxide, 9.5 mmol/L, 8:2 (v/v), as eluant.  $^{18}\text{F}$ -FDG-1,6-dP =  $^{18}\text{F}$ -FDG-1,6-diphosphate;  $^{18}\text{F}$ -FDG-6P =  $^{18}\text{F}$ -FDG-6-phosphate.

Sodium depletion had no major effect on  $^{18}\text{F}$ -FDG uptake, either in euglycemia or in hypoglycemia (Fig. 4). Glucose deprivation significantly enhanced  $^{18}\text{F}$ -FDG uptake by a factor of 2.7 ( $P < 0.02$ ; Fig. 4).

Immunocytochemical staining showed VEGF receptor-2 (KDR) on HUVECs used in this study (Fig. 5). Preincubation of HUVECs with VEGF at a concentration of 50 ng/mL had a distinct influence on  $^{18}\text{F}$ -FDG accumulation in HUVECs (Fig. 6). VEGF-treated HUVECs revealed a significantly enhanced  $^{18}\text{F}$ -FDG uptake of about 82% when compared with that of untreated control cells ( $P < 0.003$ ; Fig. 6).

$^{18}\text{F}$ -FDG uptake in HUVECs ( $70.1 \pm 40.7$  %/mg) was significantly higher than that in HMMs ( $11.7 \pm 3.6$  %/mg) and in the range of the uptake values measured in GLIOs ( $77.6 \pm 12.3$  %/mg; Fig. 7).

**TABLE 1**

Influence of Unlabeled Glucose Concentration in Incubation Buffer on  $^{18}\text{F}$ -FDG Uptake in HUVECs

Glucose concentration (mmol/L)	$^{18}\text{F}$ -FDG uptake (%/mg)
0	$59.1 \pm 8.8$
0.2	$52.9 \pm 4.0$
2	$20.8 \pm 8.4$
20	$12.2 \pm 8.5$
200	$8.9 \pm 5.9$

Uptake values are mean  $\pm$  SD of 2 independent experiments ( $n = 5$ ) obtained for HUVECs from the fourth passage (3-h incubation at  $4^\circ\text{C}$  in PBS).

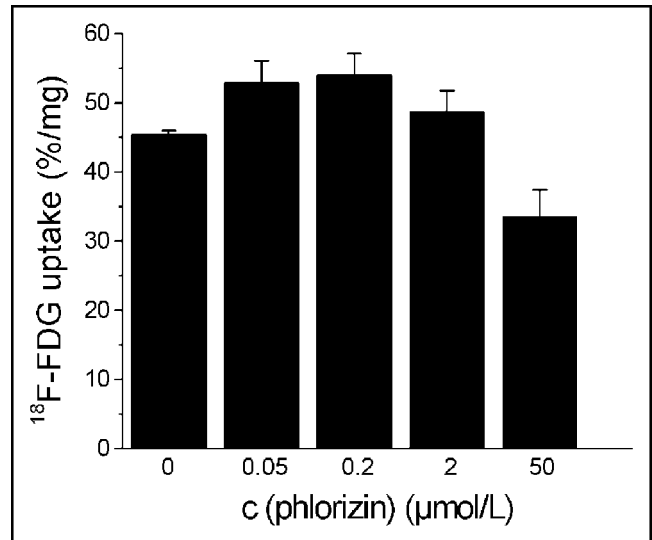


**FIGURE 2.** Influence of phlorizin on  $^{18}\text{F}$ -FDG uptake by HUVECs. Values are mean  $\pm$  SD of a single experiment performed in triplicate ( $n = 3$ ). One similar experiment yielded qualitatively identical results. c = concentration.

## DISCUSSION

The contribution of  $^{18}\text{F}$ -FDG uptake by endothelial cells to uptake values measured by PET in various tissues is as yet unclear. We therefore sought to characterize  $^{18}\text{F}$ -FDG uptake in an in vitro model of human endothelial cells.

HUVECs constitute a well-established and well-characterized model of human endothelial cells (14) and are readily available, which circumvents problems of laborious endothelial cell isolation. They are regularly used as a reference to characterize newly developed microvascular

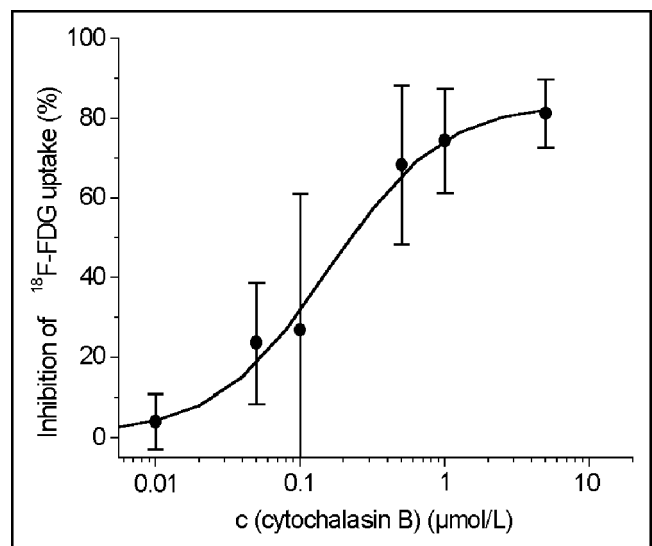


**FIGURE 3.** Inhibition of  $^{18}\text{F}$ -FDG uptake in HUVECs by cytochalasin B. Cytochalasin B competitively inhibits  $^{18}\text{F}$ -FDG uptake with an  $\text{IC}_{50}$  of  $0.16 \mu\text{mol/L}$ . Values are mean  $\pm$  COV (% of mean) of 2 independent experiments performed in triplicate ( $n = 6$ ). c = concentration.

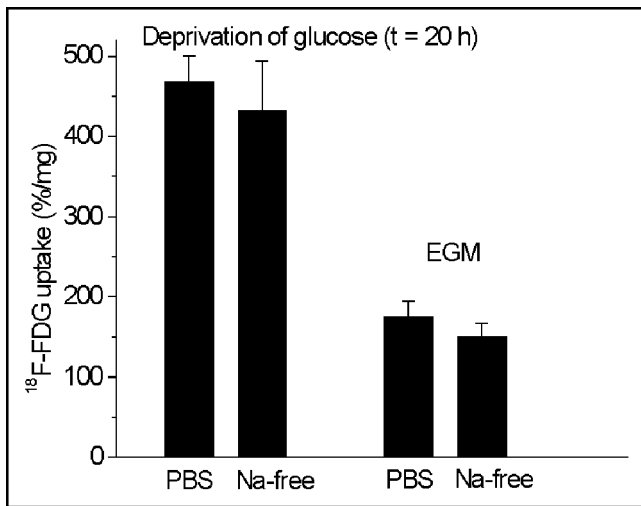


**FIGURE 4.** Influence of deprivation of glucose and sodium depletion on <sup>18</sup>F-FDG uptake in HUVECs. Glucose deprivation significantly enhances <sup>18</sup>F-FDG uptake by a factor of 2.7 ( $P < 0.02$ ). Values are mean  $\pm$  SD of a single experiment performed in triplicate ( $n = 3$ ). Two similar experiments yielded qualitatively identical results. t = time.

cell lines, such as the HMEC-1 (14). Therefore, we chose HUVECs as representative endothelial cells also in this study. However, since endothelial cells derived from different organs have been described to differ with regard to glucose metabolism (15), some caution should be applied to generalizing our observations to endothelial cells of other origin and, in particular, to those lining the blood–brain barrier as will also be discussed below.

As with other primary endothelial cultures, HUVECs have a limited life span and differ from batch to batch due to their multidonor origin. This explains some variation in uptake values in this study, ranging from 35.8 to 182.4 %/mg protein, in particular, as the variation of uptake values within single experiments had an acceptably low COV of 10%.

<sup>18</sup>F-FDG accumulated in HUVECs linearly dependent on time of incubation; furthermore, in HUVECs, <sup>18</sup>F-FDG uptake was competitively inhibited by unlabeled glucose and was a consequence of <sup>18</sup>F-FDG phosphorylation. Therefore, <sup>18</sup>F-FDG uptake by HUVECs follows mechanisms at least in principle similar to those by most other cells of the human body for which data on <sup>18</sup>F-FDG uptake are available (16). For example, in macrophages (3), radio-TLC of our cell lysates disclosed not only <sup>18</sup>F-FDG-6-phosphate but also <sup>18</sup>F-FDG-1,6-phosphate as a metabolite of <sup>18</sup>F-FDG. This is due to the acceptance of <sup>18</sup>F-FDG-6-phosphate as a substrate of phosphoglucomutase (17) and is of minor importance for PET imaging as discussed elsewhere (3).

<sup>18</sup>F-FDG uptake in HUVECs was competitively inhibited by cytochalasin B, which is a reversible inhibitor of glucose transport via the GLUT class I family comprising GLUT1–GLUT4 and also via GLUT5 (18). This interpretation receives support from studies demonstrating the expression in

particular of GLUT1 in endothelial cells obtained from human umbilical veins, whereas the placental expression of GLUT3 has been reported to be confined to the arterial component of the vascular endothelium (19). Similarly, GLUT2, GLUT4, and GLUT5 as yet have not been detected in HUVECs (15,18,19).

Recently, a second family of mammalian glucose transporters has been described in more detail, the so-called sodium glucose cotransporters (SGLTs) (16,20). These membrane proteins are able to transport glucose intracellularly using the Na<sup>+</sup>-electrochemical gradient.

SGLTs have been found in the luminal membrane of cells lining the small intestine, the proximal tubules of the kidney, and in the blood–brain barrier (18,21). The contribution of SGLTs to glucose transfer via the blood–brain barrier seems to be significant only in hypoglycemia (21).

As yet, HUVECs have not been assayed for SGLT-like transport activity. We could not establish an effect of sodium depletion on <sup>18</sup>F-FDG uptake in HUVECs, either in euglycemia or in hypoglycemia; furthermore, phlorizin, a competitive inhibitor of SGLT, had no significant effect on

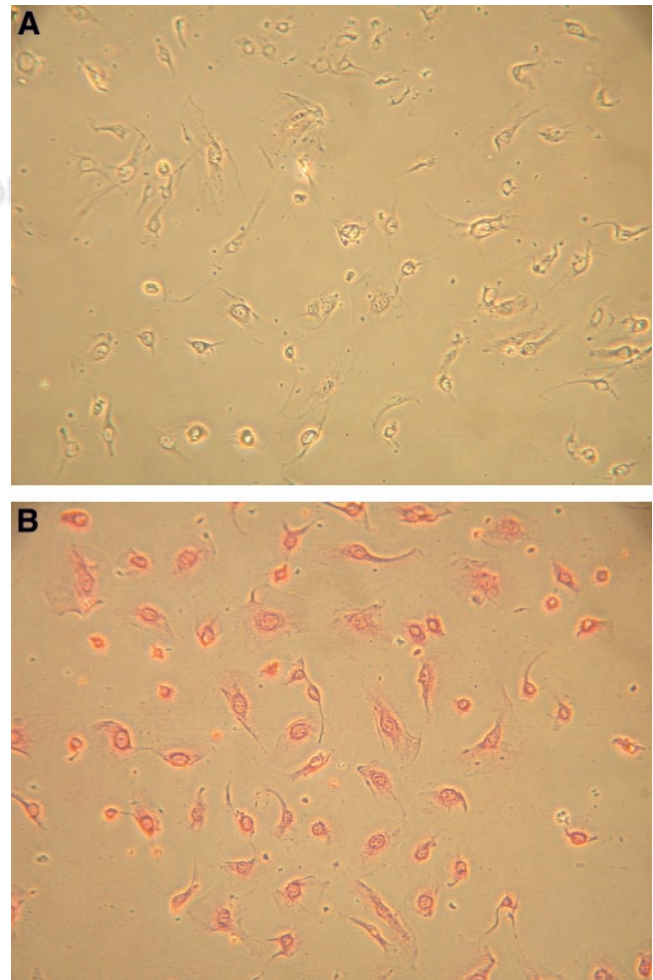


**FIGURE 5.** Immunocytochemical staining of HUVECs. Monoclonal anti-VEGF receptor-2 (KDR) was used as the primary antibody. (A) Negative control. (B) Primary antibody.

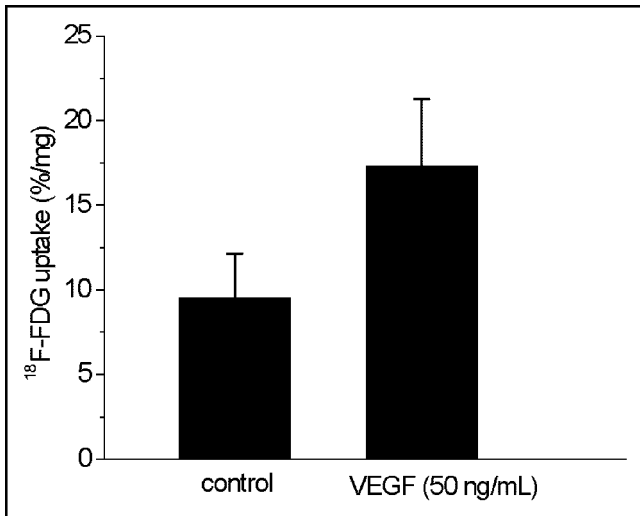


**FIGURE 6.** Influence of VEGF stimulation on <sup>18</sup>F-FDG uptake in HUVECs. HUVECs from the fourth passage were treated with VEGF (50 ng/mL, 2 h) and incubated with <sup>18</sup>F-FDG for 3 h at 4°C in PBS. Values are mean ± SD of 2 independent experiments (*n* = 6; *P* < 0.003).

<sup>18</sup>F-FDG uptake in our cell model. Therefore, in HUVECs, <sup>18</sup>F-FDG transport via Na<sup>+</sup>-dependent SGLT is negligible, if not completely absent.

The cultivation of HUVECs under hypoglycemic conditions enhances <sup>18</sup>F-FDG uptake. This has also been reported previously in cultured brain, adrenal, and aortic endothelial cells as well as in an immortalized cell line derived from primary cultures of rat brain capillary endothelial cells (22,23). Using immunoblotting or enzyme-linked immunosorbent assays, Gaposchkin and Garcia-Diaz (22) and Regina et al. (23) attributed the enhanced transport activity caused by hypoglycemia to an increased expression of GLUT1 in the cell membrane.

VEGF is a highly potent and specific inducer of angiogenesis (24,25). The 2 VEGF-receptor subtypes (Flt-1, KDR) have been described to be upregulated under hypoxic conditions or myocardial infarction (26,27). In our in vitro model, <sup>18</sup>F-FDG uptake in VEGF-treated HUVECs was significantly increased. This finding agrees with data from Sone et al., who showed that VEGF stimulated glucose transport by 69% in retinal endothelial cells (28). These authors suggest that this increase is due to protein kinase-mediated translocation of cytosolic GLUT1 to the plasma membrane surface, which might also explain the increased <sup>18</sup>F-FDG uptake in our experiments.

Under the experimental conditions of our in vitro model, <sup>18</sup>F-FDG uptake was significantly higher in HUVECs than in HMMs and in the range of the uptake values measured in GLIOs. These in vitro data can be extrapolated to in vivo conditions only with utmost caution, since they are highly dependent on the experimental setup. For example, incubation temperature was 4°C in our experimental setup, which is far below physiologic levels, as HUVECs do not stay

adherent at higher temperatures in PBS. In principle, <sup>18</sup>F-FDG uptake should be higher at higher temperatures since metabolic turnover is accelerated at higher temperatures. At 4°C, <sup>18</sup>F-FDG uptake in HUVECs was significantly higher than that in HMMs and in the same range of that in GLIOs. Nevertheless, even if we compare <sup>18</sup>F-FDG uptake measured in HUVECs at 4°C with that determined in HMMs and GLIOs at 37°C, as published previously (3), it seems justified to conclude that endothelial <sup>18</sup>F-FDG uptake is at least in the same range as that in HMMs and neoplastic cells at physiologic temperature.

Our in vitro data suggest that <sup>18</sup>F-FDG uptake in VEGF-induced endothelial cells could significantly contribute to the overall uptake values measured by <sup>18</sup>F-FDG PET in vasculitis and atherosclerosis (8,9). A more specific PET imaging tracer that takes advantage of upregulated VEGF receptors, as it was recently reported (29), could provide further insight into this issue.

Tumors also harbor VEGF-activated endothelial cells so that <sup>18</sup>F-FDG uptake values determined by PET in neoplastic tissue could also be influenced by <sup>18</sup>F-FDG uptake in endothelia. Several clinicopathologic studies have shown a direct association between VEGF expression and intratumoral microvessel density in solid tumors such as prostate, lung, and breast cancer (6). Interestingly, the expression of VEGF was linked with increased density of vessels expressing the KDR receptor (VEGF receptor-2) so that, for these types of tumors mentioned above, endothelial cell uptake of <sup>18</sup>F-FDG can possibly be expected to contribute to the overall signal.

Contrary to the possible role of inflammatory cells (2,30,31), the potential contribution of <sup>18</sup>F-FDG uptake in

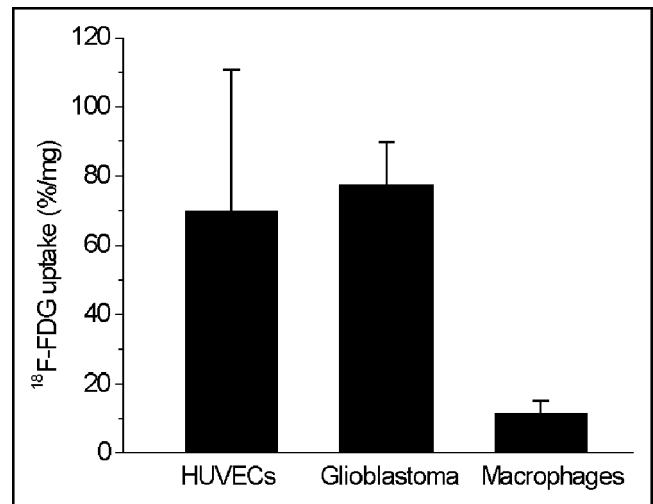


**FIGURE 7.** <sup>18</sup>F-FDG uptake in HUVECs, GLIOs, and human monocytes differentiated to macrophages (HMMs). HUVECs were from the fourth passage, HMMs differentiated to macrophages during 14 d of culture, and GLIOs were incubated for 3 h with <sup>18</sup>F-FDG at 4°C in PBS. Values are mean ± SD of multiple independent experiments: HUVECs, *n* = 22; GLIOs, *n* = 6; HMMs, *n* = 6.

endothelia to uptake values determined in neoplastic lesions has not been extensively studied as yet. Bos et al. recently reported a significant correlation between the vascularity of breast cancers and  $^{18}\text{F}$ -FDG uptake (7). However, this may not necessarily indicate a direct relationship between these variables but, rather, a correlation of both uptake and vascularity with malignancy grade. A further clarification of this issue can only be provided by in vivo studies—for example, in mouse xenotransplant models.

## CONCLUSION

$^{18}\text{F}$ -FDG accumulates in HUVECs by mechanisms analogous to those of neoplastic cells or neurons. VEGF significantly stimulates endothelial  $^{18}\text{F}$ -FDG uptake. The observed differences in  $^{18}\text{F}$ -FDG uptake between HUVECs, HMMs, and GLIOs are difficult to extrapolate to in vivo conditions but stimulate further studies on the contribution of endothelial  $^{18}\text{F}$ -FDG uptake to the overall uptake of that tracer in neoplastic or vascular lesions.

## ACKNOWLEDGMENTS

The authors thank Ulrike Ittstein for skillful laboratory assistance, Wilhelm Hamkens (PET Net GmbH, Erlangen-Tennenlohe, Germany) for providing  $^{18}\text{F}$ -FDG, and Professor Dr. Thomas Papadopoulos from the Institute of Pathologic Anatomy for helpful comments. This research was supported in part by a grant from the Deutsche Forschungsgemeinschaft, GRK 750.

## REFERENCES

- Reske S, Kotzerke J. FDG-PET for clinical use. *Eur J Nucl Med*. 2001;28:1707–1723.
- Kubota R, Yamada S, Kubota K, Ishiwata K, Tamahashi N, Ido T. Intratumoral distribution of fluorine-18-fluorodeoxyglucose in vivo: high accumulation in macrophages and granulation tissues studied by microautoradiography. *J Nucl Med*. 1992;33:1972–1980.
- Deichen JT, Prante O, Gack M, Schmiedehausen K, Kuwert T. Uptake of [ $^{18}\text{F}$ ]fluorodeoxyglucose in human monocyte-macrophages in vitro. *Eur J Nucl Med Mol Imaging*. 2003;30:267–273.
- Ishimori T, Saga T, Mamede M, et al. Increased  $^{18}\text{F}$ -FDG uptake in a model of inflammation: concanavalin A-mediated lymphocyte activation. *J Nucl Med*. 2002;43:658–663.
- Folkman J. Angiogenesis in cancer, vascular, rheumatoid and other disease. *Nat Med*. 1995;1:27–31.
- Hasan J, Byers R, Jayson GC. Intra-tumoural microvessel density in human solid tumours. *Br J Cancer*. 2002;86:1566–1577.
- Bos R, van der Hoeven JJM, van der Wall E, et al. Biologic correlates of  $^{18}\text{F}$ fluorodeoxyglucose uptake in human breast cancer measured by positron emission tomography. *J Clin Oncol*. 2002;20:379–387.
- Yun M, Jang S, Cucchiara A, Newberg AB, Alavi A.  $^{18}\text{F}$  FDG uptake in the large arteries: a correlation study with the arteriogenic risk factors. *Semin Nucl Med*. 2002;32:70–76.
- Belhocine T, Blockmans D, Hustinx R, Vandevivere J, Mortelmans L. Imaging of large vessel vasculitis with  $^{18}\text{F}$ FDG PET: illusion or reality? A critical review of the literature data. *Eur J Nucl Med Mol Imaging*. 2003;30:1305–1313.
- Pakala R, Watanabe T, Benedict CR. Induction of endothelial cell proliferation by angiogenic factors released by activated monocytes. *Cardiovasc Radiat Med*. 2002;3:95–101.
- Bradford MM. A rapid and sensitive method for the quantitation of microgram quantities of protein utilizing the principle of dye binding. *Anal Biochem*. 1976;72:248–254.
- Prante O, Hamacher K, Coenen HH. Chemo-enzymatic n.c.a. synthesis of the coenzyme uridine diphospho-2-deoxy-2-[ $^{18}\text{F}$ ]fluoro- $\alpha$ -D-glucose [abstract]. *J Labelled Compds Radiopharm*. 1999;42(suppl 1):S111–S112.
- Levene H. *Contributions to Probability and Statistics: Essays in Honor of Harold Hotelling*. Stanford, CA: Stanford University Press; 1960:278–292.
- Bouis D, Hospers GAP, Meijer C, Molema G, Mulder NH. Endothelium in vitro: a review of human vascular endothelial cell lines for blood vessel-related research. *Angiogenesis*. 2001;4:91–102.
- Mann GE, Yudilevich DL, Sobrevia L. Regulation of amino acid and glucose transporters in endothelial and smooth muscle cells. *Physiol Rev*. 2003;83:183–252.
- Gatley SJ. Labeled glucose analogs in the genomic era. *J Nucl Med*. 2003;44:1082–1086.
- Percival MD, Withers SG. Binding energy and catalysis: deoxyfluoro sugars as probes of hydrogen bonding in phosphoglucomutase. *Biochemistry*. 1992;31:498–505.
- Wood IS, Trayhurn P. Glucose transporters (GLUT and SGLT): expanded families of sugar transport proteins. *Br J Nutr*. 2003;89:3–9.
- Illsley NP. Glucose transporters in the human placenta. *Placenta*. 2000;21:14–22.
- Wright EM. Renal  $\text{Na}^+$ -glucose cotransporters. *Am J Physiol Renal Physiol*. 2001;280:F10–F18.
- Nishizaki T, Matsuoka T. Low glucose enhances  $\text{Na}^+$ /glucose transport in bovine brain artery endothelial cells. *Stroke*. 1998;29:844–849.
- Gaposchkin CG, Garcia-Diaz JF. Modulation of cultured brain, adrenal, and aortic endothelial cell glucose transport. *Biochim Biophys Acta*. 1996;1285:255–266.
- Regina A, Roux F, Revest PA. Glucose transport in immortalized rat brain capillary endothelial cells in vitro: transport activity and GLUT1 expression. *Biochim Biophys Acta*. 1997;1335:135–143.
- Sato Y, Kanno S, Oda N, et al. Properties of two VEGF receptors, Flt-1 and KDR, in signal transduction. *Ann NY Acad Sci*. 2000;902:201–205.
- Ferrara N, Gerber HP, LeCouter J. The biology of VEGF and its receptors. *Nat Med*. 2003;9:669–676.
- Brogi E, Schattman G, Wu T, et al. Hypoxia-induced paracrine regulation of vascular endothelial growth factor receptor expression. *J Clin Invest*. 1996;97:469–476.
- Li J, Brown LF, Hibberd MG, Grossman JD, Morgan JP, Simons M. VEGF, flk-1, and flt-1 expression in a rat myocardial infarct model of angiogenesis. *Am J Physiol*. 1996;270:H1803–H1811.
- Sone H, Deo BK, Kumagai AK. Enhancement of glucose transport by vascular endothelial growth factor in retinal endothelial cells. *Invest Ophthalmol Vis Sci*. 2000;41:1876–1884.
- Lu E, Wagner WR, Schellenberger U, et al. Targeted in vivo labeling of receptors for vascular endothelial growth factor: approach to identification of ischemic tissue. *Circulation*. 2003;108:97–103.
- Brown RS, Leung JY, Fisher SJ, et al. Intratumoral distribution of tritiated-FDG in breast carcinoma: correlation between Glut-1 expression and FDG uptake. *J Nucl Med*. 1996;37:1042–1047.
- Brown RS, Leung JY, Fisher SJ, Frey KA, Ethier SP, Wahl RL. Intratumoral distribution of tritiated fluorodeoxy-glucose uptake in breast carcinoma. I. Are inflammatory cells important? *J Nucl Med*. 1995;36:1854–1861.